DOI: 10.1002/ejic.200800075

A Study on the Coordinative Versatility of the Zwitterionic S,N,S Ligand $EtNHC(S)Ph_2P{=}NPPh_2C(S)NEt$ in Its Anionic, Neutral and Cationic Forms – Determination of Absolute pK_a Values in CH_2Cl_2 of Rh^I Complexes

Massimiliano Delferro,[a] Daniele Cauzzi,*[a] Roberto Pattacini,[a] Matteo Tegoni,[a] Claudia Graiff,[a] and Antonio Tiripicchio[a]

Keywords: Rhodium / Zwitterions / Coordination Modes / Acid–base properties

The coordination properties of $EtNHC(S)Ph_2P{=}NPPh_2C(S)NEt$ (HEtSNS) towards Rh^I species derived from $[Rh(CO)_2Cl]_2$ and $[Rh(cod)Cl]_2$ (cod = 1,5-cyclooctadiene) were studied. This ligand is an amphoteric zwitterion, which forms the H_2EtSNS^+ cation upon protonation and the $EtSNS^-$ dianion–cation upon deprotonation. All three forms coordinate to metal centers. Their geometrical versatility allows many coordination fashions: S-monodentate; S,S-bidentate (with a bite angle spanning from 90 to 180°); S,N,S-tridentate; N,N,N-tridentate; and S,S-bridging, as determined by X-ray diffraction methods. The [Rh(CO)EtSNS] complex is a biprotic base; its conjugated acids are $[Rh(CO)HEtSNS]^+$ and $[Rh(CO)H_2EtSNS]^{2+}$, and their pK_a values were determined in dichloromethane solutions. In this triad of compounds, which are geometrically similar, the Rh^I metal center features variable charge density as confirmed by the νCO infrared absorption frequency.

Introduction

The zwitterionic ligand $EtNHC(S)Ph_2P{=}NPPh_2NEt$ (HEtSNS, Scheme 1) can be prepared in high yield by double addition of ethylisothiocyanate (EtNCS) to bis(diphenylphosphanyl)amine ($Ph_2PNHPPh_2$, dppa),[1,2] which forms one thioamidic and one thioamidyl functionality bound to the phosphorus atoms. The opposite charges are *formally* located on the zwitterionic thioamidyl–phosphonium, $N^-C(S)P^+$, functional group. In solution, a rapid proton exchange between the thioamidic–thioamidyl functionalities is present. This exchange is facilitated by the formation of a pseudoring as a result of an intramolecular N···H···N hydrogen bond, as found in the solid-state structure.[1] Thus, the positive charge can be shared by the two P atoms of the P–N–P group and the negative charge can be delocalized on the two EtNC(S) groups (Scheme 1).

As previously reported, $EtSNS^-$ acts as an S,N,S-tridentate or S,S-bidentate ligand towards M^I species (M = Rh[1] and Cu, Ag, Au[2]). The $[-Ph_2PNPPh_2-]^+$ nitrogen atom can be coordinated as in [Rh(CO)(EtSNS)] and [Cu(EtSNS)] and it weakly interacts with the metal center in $[Ag(EtSNS)]_2$, or it can be not coordinated as in the case of [Au(EtSNS)]. The $[-Ph_2PNPPh_2-]^+$ group is reminiscent of the classical bis(triphenylphosphane)iminium cation $[Ph_3PNPPh_3]^+$ (PPN^+), whose N atom, as evidenced by its bent geometry, may coordinate a metal center, although this behavior has never been observed.[3] We also became interested in studying the coordination properties of HEtSNS and H_2EtSNS^+. Their reactivity towards Rh^I species derived from $[Rh(CO)_2Cl]_2$ and $[Rh(cod)Cl]_2$ (cod = 1,5 cyclooctadiene) is reported. Acid–base properties of the [Rh(CO)(EtSNS)] complex are discussed together with a general method for the determination of absolute pK_a values in dichloromethane.

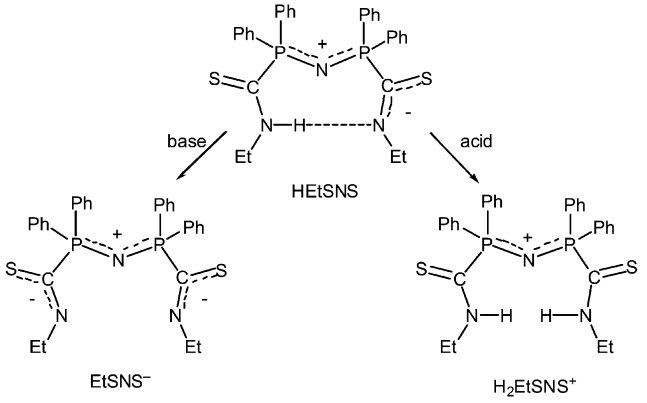

Scheme 1. Lewis structures and formal charge distribution of HEtSNS and its deprotonated ($EtSNS^-$) and protonated (H_2EtSNS^+) forms.

[a] Dipartimento di Chimica Generale ed Inorganica, Chimica Analitica, Chimica Fisica, Università degli Studi di Parma, Viale G.P. Usberti 17/A, 43100, Parma, Italy
Fax: +39-0521905557
E-mail: cauzzi@unipr.it

Supporting information for this article is available on the WWW under http://www.eurjic.org or from the author.

Results and Discussion

Acid–Base Properties of HEtSNS

The thioamidyl moiety HEtSNS can be protonated with acids such as HCl or HPF_6 to form the respective salts, whereas deprotonation of HEtSNS can be achieved with NaH (Scheme 1).

Single crystals of $(H_2EtSNS)PF_6$ (yellow) and $[Na(EtSNS)H_2O]_2$ (colorless) were obtained. Views of their crystal structures are reported in Figures 1 and 2, respectively. Selected bond lengths and angles are listed in Table 1 and compared to those previously reported for HEtSNS[1] and to those of the complexes described herein.

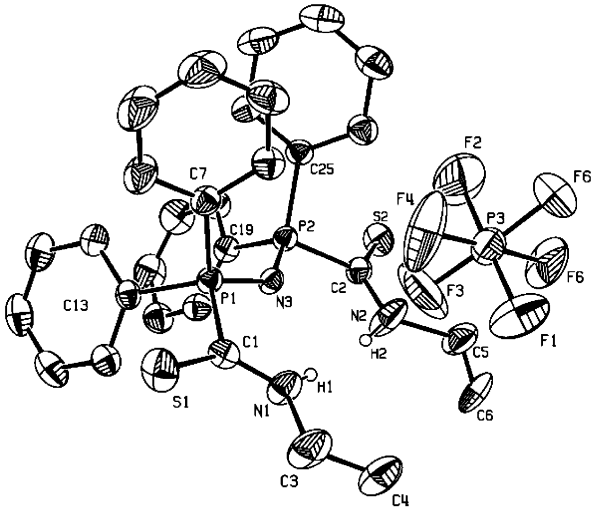

Figure 1. ORTEP plot of the molecular structure of $(H_2EtSNS)PF_6$. Thermal ellipsoids are drawn at the 30% probability level. H atoms are omitted for clarity. Only one of the two crystallographic independent $(H_2EtSNS)PF_6$, units is depicted.

In the crystals of $(H_2EtSNS)PF_6$, two independent H_2EtSNS^+/PF_6^- couples are present and display similar geometrical parameters. The N1···N2 separation of 4.315(3) Å is larger than that of HEtSNS [2.856(8) Å];[1] the latter features an intramolecular hydrogen bond (Scheme 1). Differently from HEtSNS, the P–N–P system is coplanar with the two thioamidic groups [maximum deviation from the mean plane defined by C1, N1, S1, C2, N2, S2, P1, N3, P2: 0.104 Å], probably due to a bifurcated (on the donor atom) hydrogen bonding of the type N1–H···N3···H–N2 [H1···N3 and H2···N3 distances: 2.396(1) and 2.418(1) Å]. The presence of an interaction with the N3 lone pair of electrons is also suggested by the P–N–P angle, which is significantly narrower than those of HEtSNS and $[Na(EtSNS)H_2O]_2$.

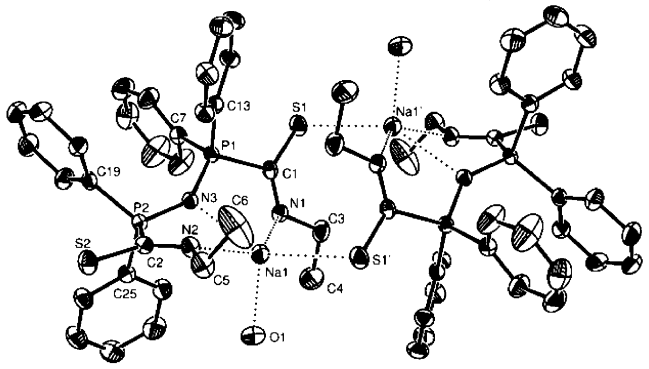

Figure 2. ORTEP plot of the structure of $[Na(EtSNS)H_2O]_2$. Thermal ellipsoids are drawn at the 30% probability level. H atoms are omitted for clarity.

The hydrated dimeric salt $[Na(EtSNS)H_2O]_2$ crystallized in air by evaporation of a CH_2Cl_2/hexane solution of [Na(EtSNS)]. Each Na^+ cation interacts with the three nitrogen atoms of $EtSNS^-$ [Na–N3, Na–N1, Na–N2 distances: 2.592(2), 2.478(2), 2.503(3) Å, respectively] and with the oxygen atom of a water molecule [Na–Ow distance: 2.277(3) Å]. The two units are connected by S···Na interactions [Na–S1′ distance is 2.893(1) Å], which results in a distorted square pyramidal geometry around Na^+. It is worthy to note that sulfur-bridged complexes of alkaline metals are far less common than their oxygen-containing counterparts.[4]

Solid Na(EtSNS) is not stable towards hydrolysis. When left in the air, it reacts with water vapor and transforms into HEtSNS. The presence of coordinated water in the crystals of $[Na(EtSNS)H_2O]_2$ seems to indicate that the dimerization results in a much lower reactivity towards hydrolysis. When a sample of Na(EtSNS) was dissolved in $CDCl_3$,

Table 1. Selected bond lengths [Å] and angles [°].

	$[Na(EtSNS)H_2O]_2$	HEtSNS	$(H_2EtSNS)PF_6$	**1**	**4**	**6**	[Rh(CO)(EtSNS)]	**8**	**7**
P1–N3	1.576(2)	1.584(2)	1.596(1)	1.5810(18)	1.5832(18)	1.580(2)	1.643(2)	1.625(2)	1.619(1)
P2–N3	1.585(2)	1.575(2)	1.599(1)	1.5798(18)	1.5721(17)	1.591(3)	1.643(2)	1.613(2)	1.619(1)
P1–C1	1.845(2)	1.841(2)	1.843(2)	1.831(3)	1.829(2)	1.843(3)	1.851(5)	1.823(3)	1.825(2)
P2–C2	1.843(2)	1.858(2)	1.837(2)	1.840(2)	1.852(2)	1.833(3)	1.851(5)	1.827(3)	1.825(2)
C1–S1	1.713(2)	1.690(2)	1.650(2)	1.747(3)	1.747(2)	1.631(3)	1.764(5)	1.742(3)	1.673(2)
C2–S2	1.705(3)	1.660(2)	1.638(2)	1.744(2)	1.656(2)	1.639(3)	1.764(5)	1.679(3)	1.673(2)
C1–N1	1.276(3)	1.297(3)	1.302(3)	1.269(3)	1.266(3)	1.305(4)	1.288(7)	1.279(3)	1.307(3)
C2–N2	1.284(3)	1.314(3)	1.291(3)	1.269(3)	1.303(3)	1.314(4)	1.288(7)	1.315(4)	1.307(3)
S1–Rh1	–	–	–	2.3457(7)	2.3614(15)	–	2.367(2)	2.315(1)	2.298(1)
S2–Rh1	–	–	–	2.4047(6)	–	–	2.367(2)	2.314(1)	2.298(1)
N–Rh	–	–	–	–	–	–	2.159(2)	2.126(2)	2.115(3)
P1–N3–P2	140.8(1)	140.3(3)	132.9(1)	136.21(12)	140.25(12)	136.71(16)	2.158(5)	2.126(2)	2.115(3)

spontaneous retransformation in H(D)EtSNS was monitored by $^{31}P\{^{1}H\}$ NMR spectroscopy over a period of ca. 2 h; the 8.0 ppm signal of colorless Na(EtSNS) was replaced by that of yellow HEtSNS at 8.4 ppm.[5] The initial observation of a sharp singlet (regardless of the temperature) suggested that, in this solution, the salt is present in its monomeric form. On the contrary, monomeric NaEtSNS is stable in DMSO solution. Also in this case, only a sharp singlet was observed in the $^{31}P\{^{1}H\}$ NMR spectrum in [D_6]DMSO (δ = 7.2 ppm) and even the addition of a large excess of water did not result in the formation of HEtSNS (δ = 13.8 ppm). This stabilizing effect probably stems from the interaction of Na^+ with DMSO through the oxygen atom.[6]

In $(H_2EtSNS)PF_6$, $[Na(EtSNS)H_2O]_2$, and HEtSNS, the P1–N3 and P2–N3 bond lengths are rather similar, whereas variations can be evidenced in the C–S and C–N distances. As expected, the protonation of the thioamidyl group results in the lengthening of the corresponding C–N bonds and in the shortening of the C–S distances; the same behavior is observed in the complexes described herein.

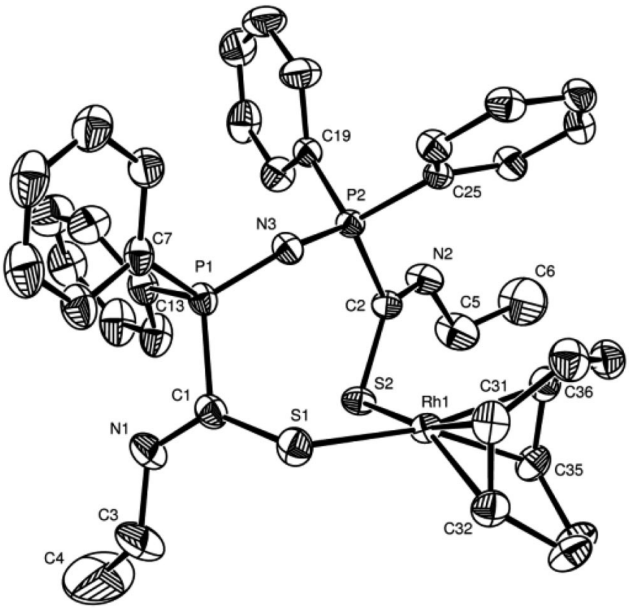

Figure 3. ORTEP plot of the molecular structure of **1**. Thermal ellipsoids are drawn at the 30% probability level. H atoms are omitted for clarity.

Coordination Properties and Geometrical Versatility of $EtSNS^-$, HEtSNS, and H_2EtSNS^+[7]

Reaction of HEtSNS with [Rh(cod)Cl]$_2$ in the Presence of tBuOK

The reaction of HEtSNS and $[Rh(cod)Cl]_2$ in the presence of a stoichiometric amount of *t*BuOK (Scheme 2) affords [Rh(cod)(*S*,*S*–EtSNS)] (**1**) in quantitative yields. A view of its molecular structure is depicted in Figure 3.

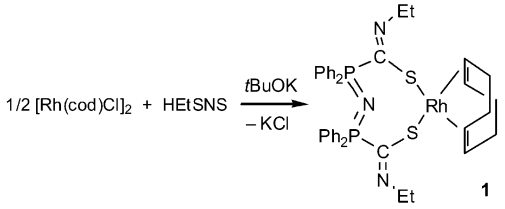

Scheme 2.

In complex **1**, $EtSNS^-$ chelates the metal center through both sulfur atoms to form an eight-membered ring. The distorted square-planar coordination is completed by a chelating cod molecule. The S1–Rh1–S2 angle of 92.90(2)° is dramatically narrower than that observed in the S,S-chelated complex [Au(EtSNS)],[2] in which the coordination over the metal center is almost linear [S1–Au1–S2 177.73(6)°]. An intermediate geometry[2] was found in dimer $[Ag(EtSNS)]_2$ [mean value of the S–Ag–S angles 136.6(1)°].[8] The structural flexibility of $EtSNS^-$ allows the ligand to comply with the coordination requests of the different metal centers. In **1**, the charge separation is conserved so that this complex belongs to the category of zwitterionic metalates.[9]

Reaction of HEtSNS with [Rh(CO)$_2$Cl]$_2$ in the Presence of tBuOK

The reaction of HEtSNS and $[Rh(CO)_2Cl]_2$ in the presence of a stoichiometric amount of *t*BuOK results in the quantitative formation of [Rh(CO)(EtSNS)]. This compound was previously reported as the product of the reaction between NaEtSNS and $[Rh(CO)_2Cl]_2$.[1b] In the same work, $[Rh(CO)_2(S,N\text{-EtSNS})]$ was proposed as an intermediate product of the reaction (evidenced by FTIR spectrophotometry). In view of the isolation of compound **1**, we now propose $[Rh(CO)_2(S,S\text{-EtSNS})]$ to be the actual intermediate, as shown in Scheme 3.

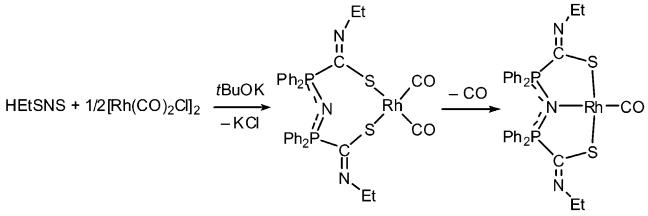

Scheme 3.

Complex **1** undergoes cyclooctadiene substitution by bubbling CO in dichloromethane solution at room temperature and atmospheric pressure, which results in its quantitative transformation into [Rh(CO)(EtSNS)].

A Rh$_2$ Dinuclear Complex

Reaction of **1** with $[Rh(cod)(thf)_2]OTf$ results in the formation of the purple dinuclear compound $[\{Rh(cod)\}_2(\mu\text{-}S,S\text{-EtSNS})]OTf$ (**2**). An ORTEP plot of the structure of $[\{Rh(cod)\}_2(\mu\text{-}S,S\text{-EtSNS})]^+$ in **2**·1/2thf is reported in Figure 4.

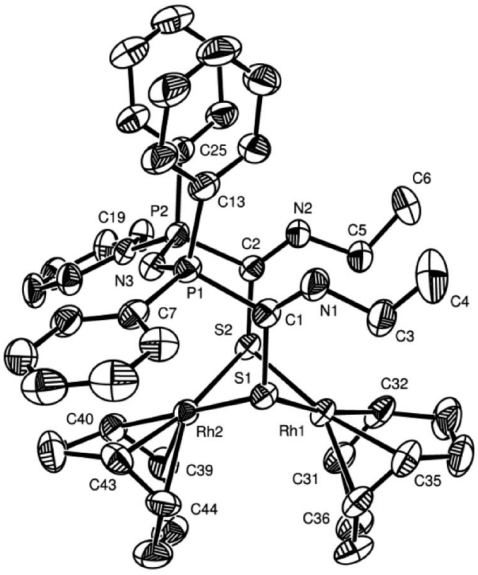

Figure 4. ORTEP plot of the molecular structure of the cation of **2** in **2**·1/2thf. Thermal ellipsoids are drawn at the 30% probability level. H atoms are omitted for clarity. Selected distances [Å] and angles [°]: P1–N3 1.591(4), P2–N3 1.587(4), P1–C1 1.834(5), P2–C21.829(5), C1–S1 1.786(5), C2–S2 1.790(5), C1–N1 1.244(6), C2–N2 1.250(6), S1–Rh1 2.417(1), S2–Rh1 2.400(1), S1–Rh2 2.369(1), S2–Rh2 2.407(2), Rh1–Rh2 2.942(1); P1–N3–P2 128.0(3).

Dinuclear complex **2** can be seen as an adduct between **1** and fragment $[Rh(cod)]^+$. Both sulfur atoms of EtSNS$^-$ bridge the metal centers to form a Rh_2S_2 core, which is rather common for dithiolate complexes.[10] The Rh–S bond lengths range from 2.369(1) Å for Rh2–S1 to 2.417(1) Å for S1–Rh1. The ligand geometry differs from that observed in compound **1**, which emphasizes its geometrical versatility. In particular, the P1, C1, S1, N1 and P2, C2, S2, N2 mean planes are almost orthogonal in **1** [88.2(1)°], whereas in **2** these planes are almost parallel [19.2(4)°].

A similar reaction between **1** and $[Rh(cod)Cl]_2$ carried out in chlorinated solvents did not afford the expected dinuclear complex [{Rh(cod)}$_2$(μ-*S*,*S*-EtSNS)]Cl (**3**), analogous to **2**, as evidenced by the $^{31}P\{^1H\}$ NMR spectra, in which only the signal of **1** (δ = 9.7 ppm, $CDCl_3$) was visible.

In contrast, **3** was quantitatively formed when methanol was used as solvent, as confirmed by $^{31}P\{^1H\}$ NMR spectroscopy and MS (ESI); the MS spectrum showed the expected $[M - Cl]^+$ peak at *m*/*z* = 980.26. The assembly of **3** was monitored by $^{31}P\{^1H\}$ spectroscopy by the addition of known quantities of CH_3OH into a stoichiometric solution of **1** and $[Rh(cod)Cl]_2$ in CD_2Cl_2 ($CD_2Cl_2/CH_3OH \approx 5$). Any attempt to obtain **3** in the solid state failed: reformation of **1** and $[Rh(cod)Cl]_2$ was observed upon solvent removal. Moreover, only crystals of the two precursors could be separated by any crystallization method that was tried. This equilibrium strongly depends on the dielectric properties of the solvent but also on the ionic strength of the solution, because upon addition of $(Et_4N)PF_6$, the assembly of **3** can be achieved in $CHCl_3$.

Reaction of HEtSNS with [Rh(cod)Cl]$_2$

The [Rh(*S*-HEtSNS)(cod)Cl] (**4**) complex, in which HEtSNS behaves as a monodentate ligand, was prepared by treating HEtSNS with $[Rh(cod)Cl]_2$ (Scheme 4).

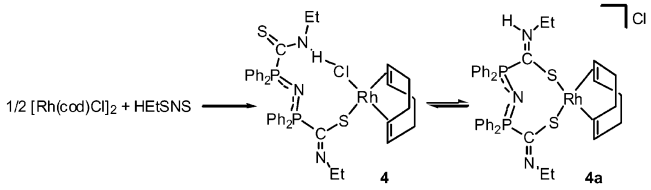

Scheme 4.

In the $^{31}P\{^1H\}$ NMR spectrum of **4** ($CDCl_3$), two sets of peaks are present. Two doublets [δ = 11.1 (d), 10.5 (d) ppm; $^2J_{P,P}$ = 15.9 Hz] can be assigned to **4**, whereas a singlet at δ = 12.4 ppm suggests the presence of a second species, probably isomer [Rh(*S*,*S*′-HEtSNS)(cod)]Cl (**4a**), which may be in slow equilibrium with **4** (integral ratio **4**/**4a** ≈ 10; see Figure S1, Supporting Information). In complex **4a**, HEtSNS could behave as an S,S-chelating ligand in a manner similar to that observed in **1**.

Isomer **4a** is only present in solution, as the HATR infrared spectrum of the crude powder obtained by evaporation of the reaction solvent was found superimposable to the spectrum of a single crystal of **4**. In the ^1H NMR spectra, two broad N–H signals can be observed at δ = 11.4 and 12.8 ppm, (assigned to **4** and **4a**, respectively). In the solid-state structure of **4**, HEtSNS is coordinated through the sulfur atom of the thioamidyl group and a chloride atom, and a chelating cod is bound to the Rh atom. An N2H3n···Cl interaction is present, which forms a 10-membered pseudoring (Figure 5).

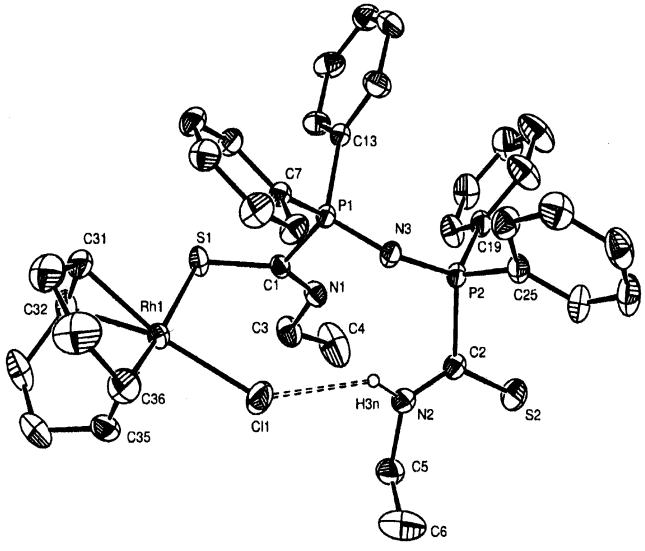

Figure 5. ORTEP plot of the molecular structure of **4**. Thermal ellipsoids are drawn at the 30% probability level. H atoms are omitted for clarity.

As evidenced by in situ $^{31}P\{^{1}H\}$ NMR spectroscopy, when *t*BuOK was added to a $CDCl_3$ solution of **4**, compound **4a** was first quickly and completely consumed, which was slowly followed by deprotonation of compound **4**. Both reactions converged to the formation of [Rh(cod)(*S*,*S*-EtSNS)] (**1**, singlet at 9.7 ppm).

This fast reactivity is in agreement with the proposed structure of **4a**, whose formula can be written as **1**·HCl.

When methanol was added to a chloroform solution of **4** (Scheme 5), the solution color instantly changed from yellow to purple. The $^{31}P\{^{1}H\}$ NMR spectrum suggested the formation of H_2EtSNS^+ along with dinuclear compound **3** (13.3 and 17.9 ppm, respectively).

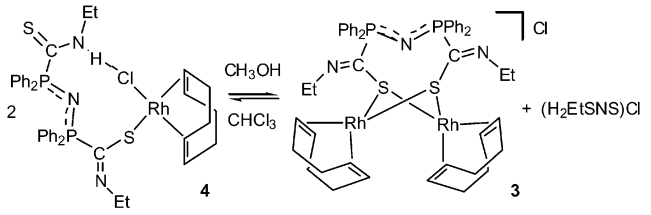

Scheme 5. Solvent dependent equilibrium for complex **3** and **4**.

This equilibrium, which implies the autoprotonation reaction: 2 HEtSNS → H_2EtSNS^+ + $EtSNS^-$ is somehow similar to the formation of **3** in methanol, which confirms that the cationic dinuclear entity [{Rh(cod)}$_2$(*μ*-*S*,*S*-EtSNS)]$^+$ is favored in polar solvents. Moreover, attempts to perform chloride abstraction from **4** by using AgOTf with the aim of obtaining a *S*,*S*′-HEtSNS chelated complex analogous to **4a** failed; this reaction only resulted in the formation of [{Rh(cod)}$_2$(*μ*-*S*,*S*-EtSNS)]OTf (**2**).

Reaction of HEtSNS with [Rh(CO)$_2$Cl]$_2$

In the reaction of HEtSNS with $[Rh(CO)_2Cl]_2$ in dichloromethane (Scheme 6), three products are formed, as detected by $^{31}P\{^{1}H\}$ NMR spectroscopy (see Figure S2, Supporting Information).

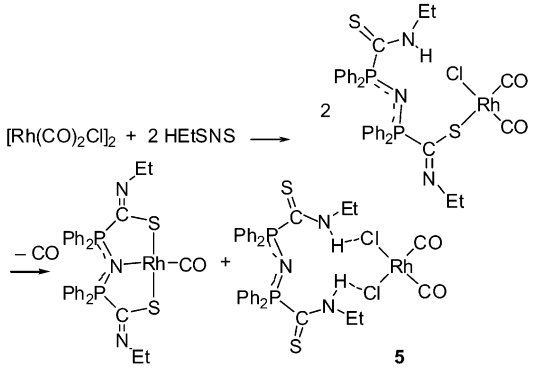

Scheme 6.

The main products of the reaction correspond to the S,N,S-tridentate complex [Rh(CO)(EtSNS)] (δ = 16.6 ppm) and [H_2EtSNS]$^+$[$Rh(CO)_2Cl_2$]$^-$ (**5**; δ = 13.3 ppm). Two low-intensity doublets at δ = 11.9 and 11.4 ppm ($^2J_{P,P}$ = 15.2 Hz) suggest the formation of the monodentate complex [Rh(CO)$_2$(*S*-HEtSNS)Cl], which is analogous to **4**, as an intermediate product. Compound **5** was separated by crystallization, and its molecular structure was determined by X-ray diffraction. The cation in compound **5** stems from the protonation reaction of HEtSNS due to the scavenging of HCl liberated in the formation of [Rh(CO)(EtSNS)]. The chloride ion was found coordinated by the Rh atom of $[Rh(CO)_2Cl_2]^-$. The reaction is probably driven by the stability of the S,N,S-tridentate complex [Rh(CO)(EtSNS)]. Complex [Rh(CO)$_2$(*S*-HEtSNS)Cl] can be regarded as the first reaction product, which successively yields **5** and [Rh(CO)(EtSNS)]. An ORTEP view of the X-ray molecular structure of **5** is reported in Figure S3 (Supporting Information), and it displays geometrical parameters analogous to those observed for compound **6** (vide infra).

Reaction of (H$_2$EtSNS)X (X = Cl, PF$_6$) with [Rh(cod)Cl]$_2$

The reactivity of (H_2EtSNS)X (X = Cl, PF_6) depends on the coordinative properties of the anion. The reaction of (H_2EtSNS)Cl with $[Rh(cod)Cl]_2$ yielded [H_2EtSNS]-[$Rh(cod)Cl_2$] (**6**). A view of its molecular structure, determined by X-ray diffraction methods, is reported in Figure 6.

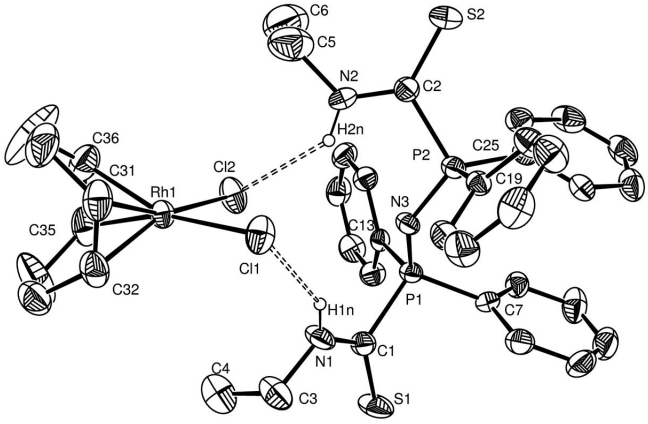

Figure 6. ORTEP plot of the molecular structure of **6**. Thermal ellipsoids are drawn at the 30% probability level. H atoms are omitted for clarity.

In the crystal structure, bond lengths and angles of H_2EtSNS^+ are similar to those observed for (H_2EtSNS)-PF_6, except for the P–N–P angle, which is slightly bigger [**6**: 136.7(2)°; (H_2EtSNS)PF_6: 132.9(1), 133.9(1)°], and the value of the C1–P1–P2–C2 torsion angle [ca. 1° for (H_2EtSNS)PF_6 and 91° for **6**]. The cation–anion interaction features two NH···Cl hydrogen bonds as depicted in Figure 6. The positive charge is located on the P–N–P system, and this interaction is reminiscent of the anion coordination by neutral thioureas and ureas.[11] No reaction was observed between (H_2EtSNS)PF_6 and $[Rh(cod)Cl]_2$. The H_2EtSNS^+ cation is thus unable to open the chloride bridge of the dimeric precursor and coordinate to the Rh center (see below for the coordination properties of H_2EtSNS^+).

Reaction of $(H_2EtSNS)X$ (X = Cl, PF_6) with $[Rh(CO)_2Cl]_2$

Although **6** can be quantitatively prepared by the aforementioned reaction of $(H_2EtSNS)Cl$ with $1/2[Rh(cod)Cl]_2$, a similar reaction pathway cannot be followed for the synthesis of **5**.

The reaction of $(H_2EtSNS)Cl$ with $[Rh(CO)_2Cl]_2$ in CH_2Cl_2 afforded $[Rh(CO)(S,N,S\text{-}H_2EtSNS)][Rh(CO)_2Cl_2]_2$ (**7**); two unreacted $(H_2EtSNS)Cl$ molecules were also observed by $^{31}P\{^1H\}$ NMR spectroscopy. The coordination of the Cl^- ion liberated in the formation of $[Rh(CO)(S,N,S\text{-}H_2EtSNS)]^{2+}$ afforded the two chloridorhodates $[Rh(CO)_2Cl_2]^-$ and, due to the formation of a new coordination site by the loss of a CO molecule, the H_2EtSNS^+ cation could act as ligand for a $Rh(CO)^+$ group. A more convenient preparation of **7** was achieved by treating $(H_2EtSNS)Cl$ with $[Rh(CO)_2Cl]_2$ in a 2:3 ratio (Scheme 7). A view of its structure, determined by X-ray diffraction methods, is reported in Figure 7.

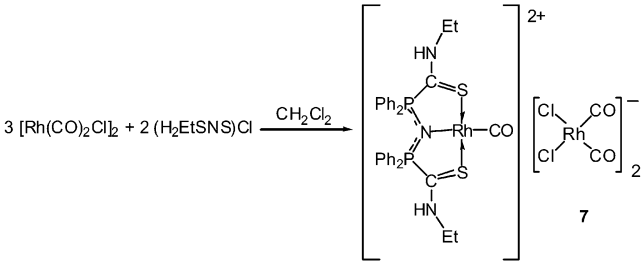

Scheme 7.

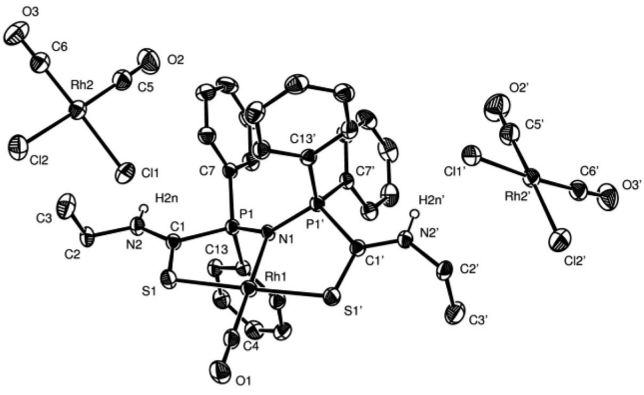

Figure 7. ORTEP plot of the molecular structure of **7**. Thermal ellipsoids are drawn at the 30% probability level. H atoms are omitted for clarity. Symmetry transformation used to generate equivalent atoms: $1 - x$, y, $1/2 - z$.

The formation of **7** suggested that other stable protonated derivatives of [Rh(CO)(EtSNS)] could be obtained (Scheme 8). Indeed, $[Rh(CO)(S,N,S'\text{-}HEtSNS)]PF_6$ ($[Rh(CO)(EtSNS)]\cdot HPF_6$, **8**) was synthesized by protonation of [Rh(CO)(EtSNS)] with an equimolar amount of HPF_6 or by complexation of $[Rh(CO)_2(MeCN)_2]PF_6$ with HEtSNS. In a similar manner, $[Rh(CO)(S,N,S\text{-}H_2EtSNS)](PF_6)_2$ ($[Rh(CO)(EtSNS)]\cdot 2HPF_6$, **9**) was prepared by protonation of [Rh(CO)(EtSNS)] with two equimolar amounts of HPF_6 or by treating $[Rh(CO)_2(MeCN)_2]PF_6$ with $(H_2EtSNS)PF_6$. The latter reaction is an example of complex formation by treating a cationic ligand with a cationic metal fragment, which is not frequent in coordination chemistry.[12] The cations of **7** and **9**, $[Rh(CO)(S,N,S\text{-}H_2EtSNS)]^+$, are identical. Single crystals of **8**·2thf were obtained. Its structure is depicted in Figure 8.

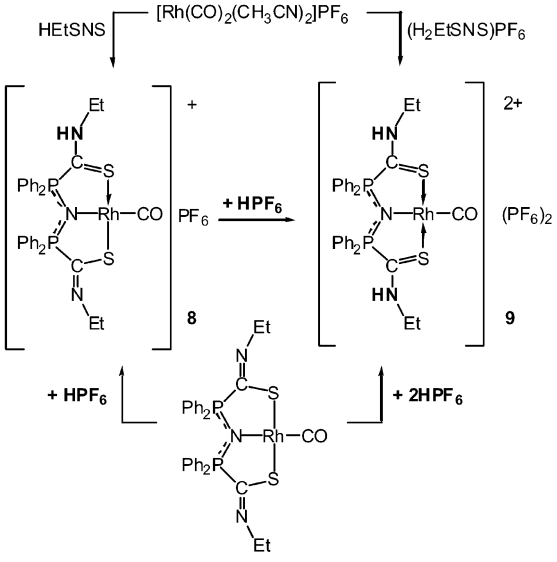

Scheme 8. Formation of complexes **8** and **9** by protonation of [Rh(CO)EtSNS] and direct complexation of $[Rh(CO)]^+$ species.

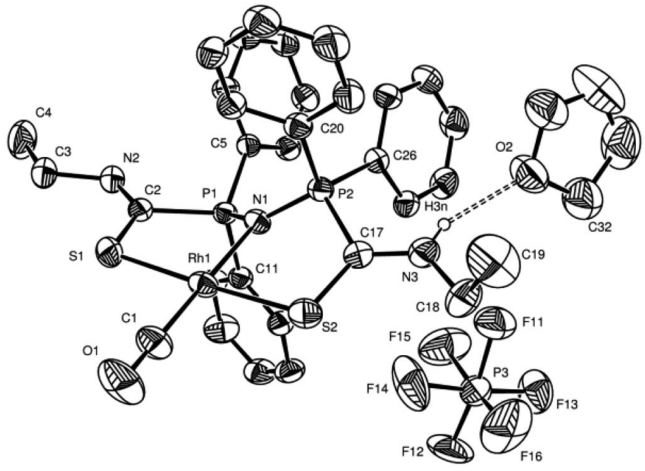

Figure 8. ORTEP plot of the molecular structure of **8**·thf in **8**·2thf. Thermal ellipsoids are drawn at the 30% probability level. H atoms are omitted for clarity. The second thf molecule was not involved in interactions with the complex and is omitted for clarity.

It is worthy to note that in **7**, **8**, and [Rh(CO)(EtSNS)], the coordination geometry is almost identical. The ligands correspond to, respectively, cationic H_2EtSNS^+, neutral–zwitterionic HEtSNS, and dianionic–cationic $EtSNS^-$. In the solid state infrared HATR spectra of [Rh(CO)(EtSNS)], **8**, and **9**, the CO stretching frequency increases (1951, 1979, and 1996 cm^{-1}, respectively, in the solid state; 1968, 1994, and 2017 cm^{-1}, respectively, in CH_2Cl_2 solution), which

suggests that the protonation of [Rh(CO)(EtSNS)] results in a decreased electron density on the metal center and thus in a weaker Rh→CO back donation.[13] The P–N distances in **7** and **8** are slightly shorter than those of [Rh(CO)-(EtSNS)], as well as the P–C ones. Because the protonation of HEtSNS does not affect the P–N–P system (see Table 1), this small change could result from variations in the ligating properties of the thioamidyl/thioamidic groups. In fact, the Rh–S bond length increases in the **7**, **8**, and [Rh(CO)-(EtSNS)] series, which in turn affects the P–N–P system through the metal center. The thioamidyl fragment, which is more thiolato in character, is a stronger donor than the thioamidic group of thione character. The Rh–N distance is slightly shorter in the protonated species, which is probably influenced by the lower electron density on the Rh atom. The $^{31}P\{^{1}H\}$ NMR chemical shift is strongly affected by the protonation: [Rh(CO)(EtSNS)] shows a sharp singlet at δ = 16.6 ppm ($CDCl_3$), whereas in **9** the two equivalent P atoms resonate at δ = 38.2 ppm. The $^{31}P\{^{1}H\}$ NMR spectroscopic data recorded in $CDCl_3$ for **8** show two sharp singlets (35.0 and 19.9 ppm) assigned, respectively, to the P atoms bound to the thioamidic and thioamidyl coordinated functionalities,[14] which is suggestive of the absence of fast proton exchange. The solid state $^{31}P\{^{1}H\}$ NMR-MAS spectrum of compound **8** was recorded and two peaks (36.1 and 24.1 ppm) were observed. As a reference, in the solid-state NMR spectrum of HEtSNS, two singlets are found at 8.1 (thioamidic) and 2.6 ppm (thioamidyl), which shows that Rh coordination exerts a strong influence on the chemical shift of the P atoms. The formal Lewis structures depicted in Scheme 8 are in agreement with this observation and with the bond lengths discussed above. The thioamidic groups can be considered neutral in **8** and **9**; the *formal* charge on the Rh atom is negative in [Rh(CO)(EtSNS)], neutral in **8**, and positive in **9**. The Mulliken atomic net charge for complex [Rh(CO)(EtSNS)] (–0.150, –0.157, –0.177 in the gas phase, in cyclohexane, and in thf, respectively) was calculated by DFT methods.[1a] A positive charge is always shared by the two P atoms.

Protonation Reaction of Complex 1

The protonation behavior of complex **1** in the presence of HCl or HOTf does not parallel that of [Rh(CO)EtSNS]; a change in the ligand coordination geometry was observed, as depicted in Scheme 9. When one equivalent of HCl was used, S-monodentate HEtSNS was formed, and the chloride anion substituted a sulfur atom in the coordination sphere of Rh to yield complexes **4** and **4a**. With two equivalents of HCl, the H_2EtSNS^+ cation formed and the second chloride anion entered into the coordination sphere of Rh to yield complex **6**. When HOTf was used, the formation of **2** was observed, together with one equivalent of H_2EtSNS^+. The different reactivity is apparently due to the lower stability of the bidentate complex with respect to the tridentate [Rh(CO)EtSNS].

Acid–Base Properties of [Rh(CO)(EtSNS)]

Protonation equilibria of [Rh(CO)(EtSNS)] were studied by means of spectroscopic UV/Vis titration in CH_2Cl_2 by using a solution of HOTf in a 1.5% mixture of methanol in dichloromethane.[15] Under these conditions it was assumed that HOTf is completely dissociated and acts as a superacid[16] so that the concentration of H^+ can be considered equal to the analytical concentration of the acid added (the methanol is present to allow the triflic acid to completely dissolve and to level HOTf to $CH_3OH_2^+$).[16b] These circumstances allow for the determination of the pK_a in this solvent on an absolute scale. In the literature, protonation equilibria of ligands and complexes in CH_2Cl_2 were studied by means of proton exchange reactions by using $HP(Cy)_3^+$ (Cy = cyclohexyl) as a weak acid, for which a pK_a = 9.7

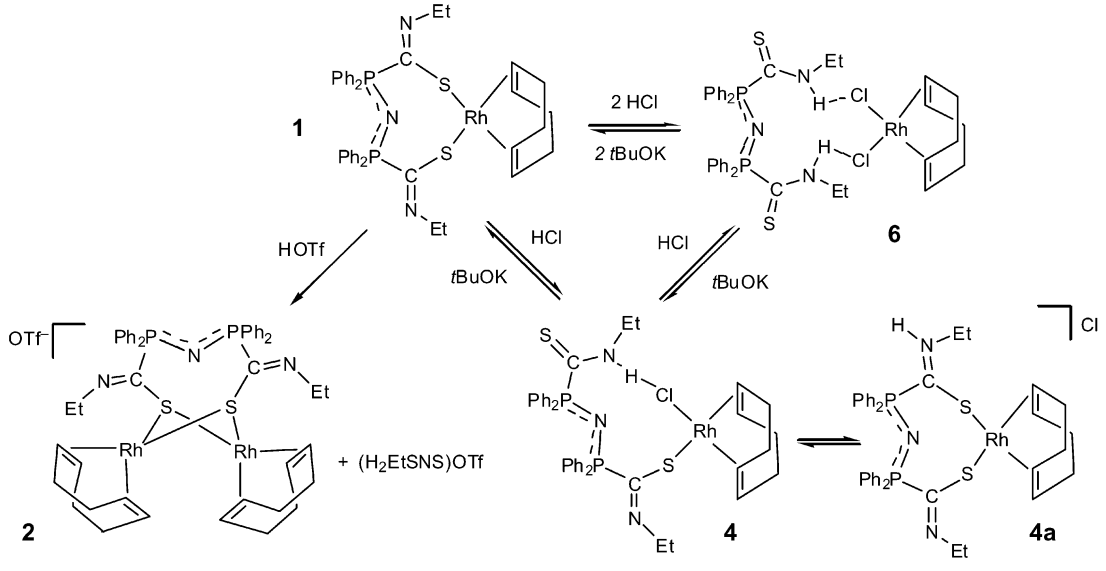

Scheme 9. Acid–base reactions for complex **1**.

was established by literature convention.[17] This pK_a scale, however, represents a relative pK_a ladder that should be rescaled to the real $HP(Cy)_3^+$ acidity constant.[18] The employment of triflic acid as titrant, dissolved in CH_2Cl_2 with small amounts of methanol, allows direct evaluation of protonation equilibria in a similar way as studying the protonation equilibria in water by means of fully dissociated HCl.

In the titration of [Rh(CO)(EtSNS)] with triflic acid, three very well-defined isosbestic points were detected: one at 438 nm for acid to complex ratios from 0 to 1 and two at 509 and 385 nm for acid to complex ratios from 1 to 2 (Figure 9). These results are in agreement with the expected diprotic nature of $[Rh(CO)(H_2EtSNS)]^{2+}$ and the presence of two distinct protonation processes involving [Rh(CO)(EtSNS)].

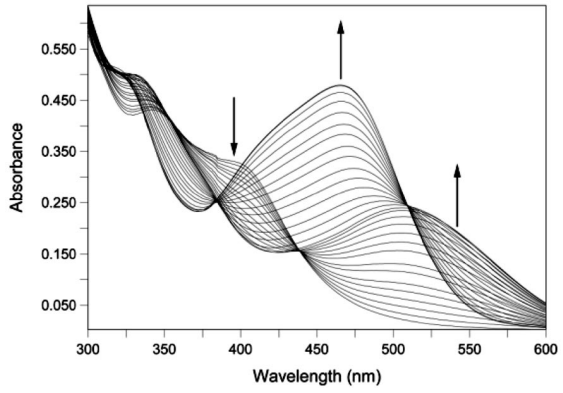

Figure 9. UV/Vis spectra (300–600 nm) for the titration of [Rh(CO)(EtSNS)] with HOTf in CH_2Cl_2.

Two pK_a values of 4.8(4) and 6.5(3) ($\sigma = 4.11 \times 10^{-2}$) were determined for the dissociation processes:

$[Rh(CO)(H_2EtSNS)]^{2+} \rightleftharpoons [Rh(CO)(HEtSNS)]^{+} + H^{+}$

$[Rh(CO)(HEtSNS)]^{+} \rightleftharpoons [Rh(CO)(EtSNS)] + H^{+}$

A representative distribution diagram for the $[Rh(CO)(H_2EtSNS)]^{2+}$ complex is shown in Figure 10 {UV spectra of pure samples of [Rh(CO)(EtSNS)], [Rh(CO)(EtSNS)]·HOTf and [Rh(CO)(EtSNS)]·2HOTf are reported in the Supporting Information}. Recently, a similar acid–base behavior was observed for Pd complexes of thioamidic SNS pincer ligands but protonation constants were not determined.[19] Unfortunately, although the protonation equilibria of several complexes were investigated in the last decade[16,17] the dissociation constants were all referenced to the $HP(Cy)_3^+$ standard, and no direct comparison with those values is possible. Titration of HEtSNS by UV/Vis was not possible due to the absence of suitable variations in the absorption spectra. The titration was performed by monitoring the protonation by ^{31}P NMR spectroscopy. Under these conditions, the basicity of the ligand is too high for pK_a determination.

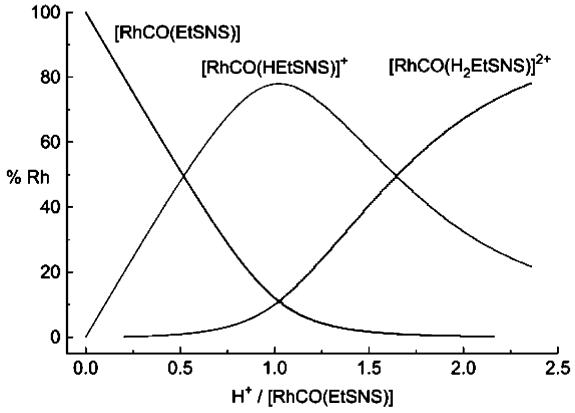

Figure 10. Distribution diagram for the titration of [Rh(CO)(EtSNS)] ($C_{Rh} = 1 \times 10^{-4}$ M).

Conclusions

The zwitterionic ligand HEtSNS is amphoteric and possesses ligating properties in all of its three forms: zwitterionic–neutral, zwitterionic–anionic, and cationic. This work, together with previous results, evidenced its geometrical versatility, which allows the following coordination fashions: *S*-monodentate (compound **4**); eight-membered chelating *S*,*S*-bidentate with 180° bite-angle ([Au(EtSNS)][2]) or 90° bite-angle (compound **1**); S,N,S-bis(chelating) ([Rh(CO)EtSNS],[1] [Cu(EtSNS)][2]); and N,N,N-tridentate coordination in $[Na(EtSNS)H_2O]_2$, in which monodentate S-coordination is also found. The S atoms are also able to bridge as in clusters described in ref.[2] and in dinuclear complex **2**. In the case of $[Rh(cod)]^+$ precursors, the coordination geometry and complex nuclearity in solution are strongly dependent on the polarity of the solvent. Noteworthy, HEtSNS, $EtSNS^-$, and H_2EtSNS^+ show the same S,N,S-coordinating properties towards the cationic metal species $[Rh(CO)]^+$ {compounds [Rh(CO)EtSNS], **7**, **8**, and **9**, respectively). Protonated complexes can be prepared also by reaction of acids with [Rh(CO)EtSNS], whose two pK_a have been determined in CH_2Cl_2 solution. The protonation causes a change in the electron density on the Rh atom, as evidenced by the stretching vibration of the coordinated CO molecule, which could be exploited in tuning its catalytic properties, for instance in reactions involving oxidative addition on the metal center.

Experimental Section

General Procedure and Materials: All manipulations were carried out at room temperature in air or, when necessary, under a nitrogen atmosphere by standard Schlenk techniques. *t*BuOK, EtNCS, $[Rh(cod)Cl]_2$, $[Rh(CO)_2Cl]_2$, $AgPF_6$, AgOTf (OTf = CF_3SO_3), HOTf, HPF_6 (60% aqueous solution), and NaH were purchased and used as received (Aldrich and Fluka). The solvents was dried and distilled by standard techniques. $Ph_2PNHPPh_2$ (dppa),[20] HEtSNS,[1] $(H_2EtSNS)Cl$,[1] [Rh(CO)(EtSNS)],[2] $[Rh(CH_3CN)_2(CO)_2]X$, and $[Rh(thf)_2(CO)_2]X$ ($X = PF_6^-$, OTf^-)[21] were prepared as described elsewhere. Elemental analyses were carried out with a Carlo Erba EA1108 microanalyzer. FTIR spectra (4000–400 cm^{-1}) were recorded with a Nicolet Nexus spectrophotometer equipped with a Smart Orbit HATR accessory (diamond crystal). ^1H NMR (300.13 MHz, TMS) and $^{31}P\{^1H\}$ NMR (161.98 MHz, external

reference 85% H_3PO_4) spectra were recorder with Bruker instruments (AC300 Avance and AMX400, respectively) by using deuterated solvents ($CDCl_3$, CD_2Cl_2, [D_6]DMSO, and CD_3OD). The solid-state $^{31}P\{^1H\}$NMR-MAS spectra were recorded with a Bruker Avance 300 MHz operating at a frequency of 121.57 MHz and equipped with a MAS 4 mm ^1H-X probe. Sample rotation was set at 1010 Hz. $NH_4H_2PO_4$ was used as an external reference (δ = 0 ppm), and PF_6^- (–144 ppm) was used as an internal secondary reference. A Micromass Quattro LC triple quadrupole instrument equipped with an electrospray interface (Masslynx v. 3.4 software) was used for MS data collection and processing. The nebulizing gas (nitrogen, 99.999% purity) and the desolvation gas (nitrogen, 99.998% purity) were delivered at a flowrate of 80 and 500 L h^{-1}, respectively. MS (ESI) analyses were performed by operating the mass spectrometer in positive ion (PI) mode and by acquiring mass spectra over the scan range *m*/*z* 100–2800 with a step size of 0.1 Da and a scan time of 2.7 s. The interface operating parameters were: source temperature 70 °C, desolvation temperature 70 °C, ESI(+) capillary voltage 3.0 kV, cone voltage 15 V, rf lens 0.3 V. Absorption spectra in the range 300–600 nm were recorded with a Perkin–Elmer Lambda 25 spectrophotometer by using matched quartz cells of 1 cm path length and dichloromethane as reference.

[Na(EtSNS)]: A suspension of NaH (0.043 g, 1.79 mmol) in thf (20 mL) was added to a solution of HEtSNS (0.500 g, 0.89 mmol) in thf (20 mL) under an atmosphere of nitrogen. The resulting suspension was stirred for 1 h. Unreacted NaH was removed by filtration. Evaporation of the solvent afforded [Na(EtSNS)] as a white powder (Yield: 97%). [Na(EtSNS)] was recrystallized by slow evaporation of a CH_2Cl_2/hexane solution to yielding [Na(EtSNS)-H_2O]$_2$. ^1H NMR (300.13 MHz, [D_6]DMSO): δ = 8.0–7.2 (m, 20 H, Ph), 3.42 (qd, $^3J_{H,H}$ = 7.2 Hz, $^4J_{H,P}$ = 5.0 Hz, 4 H, CH_2CH_3), 0.99 (t, $^3J_{H,H}$ = 7.2 Hz, 6 H, CH_2CH_3) ppm. $^{31}P\{^1H\}$ NMR (161.98 MHz, [D_6]DMSO): δ = 7.2 (s) ppm. $C_{30}H_{30}N_3NaP_2S_2$ (581.65): calcd. C 61.95, H 5.20, N 7.22, S 11.03; found C 62.31, H 5.31, N 7.25, S 10.87.

(H_2EtSNS)PF_6: Solid HEtSNS (0.073 g, 0.13 mmol) was dissolved in CH_2Cl_2 (10 mL), which resulted in a yellow solution; a solution of HPF_6 (60% in H_2O, 0.2 mL, 2.4 mmol) was added, and the reaction mixture was vigorously shaken. The aqueous phase was removed, and the resulting organic phase was dried with anhydrous Na_2SO_4 and evaporated under reduced pressure to obtain (H_2EtSNS)PF_6 as a yellow powder (Yield: 98%). ^1H NMR (300.13 MHz, $CDCl_3$): δ = 12.8 (s, 2 H, N-H), 8.0–7.3 (m, 40 H, Ph), 4.05 (qd, $^3J_{H,H}$ = 7.2 Hz, $^4J_{H,P}$ = 5.0 Hz, 4 H, CH_2CH_3), 1.41 (t, $^3J_{H,H}$ = 7.2 Hz, CH_2CH_3) ppm. $^{31}P\{^1H\}$ NMR (161.98 MHz, $CDCl_3$): δ = 13.3 (s) ppm. $C_{30}H_{32}F_6N_3P_3S_2$ (705.64): calcd. C 51.06, H 4.57, N 5.95, S 9.09; found C 52.03, H 4.62, N 6.15, S 9.54.

[Rh(cod)(*S*,*S*-EtSNS)] (1): Solid [Rh(cod)Cl]$_2$ (0.100 g, 0.203 mmol) and HEtSNS (0.226 g, 0.406 mmol) were dissolved in CH_2Cl_2 (10 mL). A solution of *t*BuOK (0.046 g, 0.406 mmol) in MeOH (2 mL) was then added, and the reaction mixture was stirred for 30 min. The volatiles were evaporated, and the resulting yellow powder was redissolved in CH_2Cl_2 (5 mL). KCl was removed by filtration. Evaporation of the solvent afforded **1** as a yellow powder (Yield: 85%). Complex **1** could be recrystallized by layering hexane onto a CH_2Cl_2 solution. ^1H NMR (300.13 MHz, $CDCl_3$): δ = 7.8–7.2 (m, 20 H, Ph), 3.9–3.7 (m, 4 H, CH=CH, cod; m, 4 H, CH_2CH_3), 1.87 (br., 4 H, C*H*H, cod), 1.52 (m, 4 H, CH*H*, cod), 1.18 (t, $^3J_{H,H}$ = 7.1 Hz, 6 H, CH_2CH_3) ppm. $^{31}P\{^1H\}$ NMR (161.98 MHz, $CDCl_3$): δ = 9.7 (s) ppm. $C_{38}H_{42}N_3P_2RhS_2$ (769,74): calcd. C 59.29, H 5.50, N 5.46, S 8.33; found C 59.11, H 5.64, N 5.29, S 8.16.

[{Rh(cod)}$_2$(μ-*S*,*S*-EtSNS)]OTf (2): A solution of AgOTf (0.077 g, 0.30 mmol) in thf (10 mL) was added dropwise to a solution of [Rh(cod)Cl]$_2$ (0.075 g, 0.15 mmol) in thf (10 mL). The resulting reaction mixture was stirred at room temperature for 10 min. Solid AgCl was removed by filtration. To this solution was added complex **1** (0.115 g, 0.15 mmol), and the purple reaction mixture was stirred for 1 h. Evaporation of the volatiles yielded **2** as a purple powder (Yield: 76%). The complex can be recrystallized by layering hexane onto a thf solution to afford violet crystals of **2**·1/2thf. ^1H NMR (300.13 MHz, $CDCl_3$): δ = 7.7–7.2 (m, 20 H, Ph), 4.20 (dq, $^3J_{H,H}$ = 7.2 Hz, $^4J_{H,P}$ = 4.2 Hz, 4 H, CH_2CH_3), 4.23 (br., 4 H, CH=CH, cod), 3.73 (s, 4 H, CH=CH, cod), 2.42 (br., 8 H, C*H*H, cod), 1.95 (m, 8 H, CH*H*, cod), 1.45 (t, $^3J_{H,H}$ = 7.2 Hz, 6 H, CH_2CH_3) ppm. $^{31}P\{^1H\}$ NMR (161.98 MHz, $CDCl_3$): δ = 17.9 (s) ppm. $C_{47}H_{54}F_3N_3O_3P_2Rh_2S_3$ (1129.90): calcd. C 49.96, H 4.82, N 3.72, S 8.51; found C 50.12, H 4.83, N 3.63, S 8.74. MS (ESI+, CH_2Cl_2): *m*/*z* (%) = 980.26 (100) [M]$^+$.

Reaction of 1 with [Rh(cod)Cl]$_2$ To Form [{Rh(cod)}$_2$(μ-*S*,*S*-EtSNS)]Cl (3): A solution of [Rh(cod)Cl]$_2$ (0.024 g, 0.097 mmol) in CH_2Cl_2 (10 mL) was added to a solution of **1** (0.150 g, 0.195 mmol) in CH_2Cl_2 (10 mL). The resulting orange reaction mixture was stirred for 10 min. Methanol (40 mL) was added, and the solution color turned to purple. Evaporation of the solvent yielded the starting mixture of the reagents. The same reaction was performed in CD_3OD in order to obtain NMR spectroscopic data for **3**. ^1H NMR (300.13 MHz, CD_3OD): δ = 7.5–7.2 (m, 20 H, Ph), 4.21 (m, 4 H, CH_2CH_3, m, 4 H, CH=CH, cod), 3.7 (s, 4 H, CH=CH, cod), 2.40 (s, 8 H, CH*H*, cod), 1.95 (m, 8 H, C*H*H, cod), 1.45 (t, 6 H, CH_2CH_3) ppm. $^{31}P\{^1H\}$ NMR (161.98 MHz, CD_3OD): δ = 17.1 (s) ppm. MS (ESI+, MeOH): *m*/*z* (%) = 980.26 (100) [{Rh(cod)}$_2$(μ-*S*,*S*-EtSNS)]$^+$.

[Rh(cod)(*S*-HEtSNS)Cl] (4): A solution of HEtSNS (0.145 g, 0.26 mmol) in CH_2Cl_2 (20 mL) was added to a solution of [Rh(cod)-Cl]$_2$ (0.064 g, 0.13 mmol) in CH_2Cl_2 (10 mL). The red reaction mixture was stirred for 10 min. Evaporation of the solvent yielded **4** as a yellow powder (Yield: 92%), which could be recrystallized by layering hexane onto a CH_2Cl_2 solution. In solution, compound **4** was found to be in equilibrium with [Rh(cod)(*S*,*S*′-HEtSNS)]Cl (**4a**). Data for **4**: ^1H NMR (300.13 MHz, $CDCl_3$): δ = 11.37 (br. s, N-H), 7.7–7.2 (m, Ph), 4.15 (br. m, C*H*=C*H*, cod), 4.00 (br. m, CH_2CH_3), 3.93 (br. m, CH_2CH_3), 3.63 (br. m, CH=CH, cod), 2.13 (br. s, C*H*H, cod), 1.48 (m, CH*H*, cod), 1.27 (t, $^3J_{H,H}$ = 6 Hz, CH_2CH_3) ppm. signals of compound **4a** (except for NH group) were underimposed to signals of compound **4** thus affecting peak integration.$^{31}P\{^1H\}$ NMR (161.98 MHz, $CDCl_3$): δ = 11.1 (d, $^2J_{P,P}$ = 15.9 Hz), 10.5 (d, $^2J_{P,P}$ = 15.9 Hz) ppm. $C_{38}H_{43}ClN_3P_2RhS_2$ (806.21): calcd. C 56.61, H 5.38, N 5.21, S 7.95; found C 57.46, H 5.46, N 5.37, S 8.10. Data for **4a**: $^{31}P\{^1H\}$ NMR (161.98 MHz, $CDCl_3$): δ = 12.4 (s, integral ratio with respect to complex **4** = 1:10) ppm. ^1H NMR (300.13 MHz, $CDCl_3$): δ = 12.82 (br. s, N-H) ppm.

Reaction of [Rh(CO)$_2$Cl]$_2$ with HEtSNS: A solution of HEtSNS (0.280 g, 0.50 mmol) in CH_2Cl_2 (10 mL) was added under an atmosphere of nitrogen to [Rh(CO)$_2$Cl]$_2$ (0.097 g, 0.25 mmol) dissolved in CH_2Cl_2 (15 mL). The solution color changed rapidly from yellow to red. Stirring was continued for 2 h, and the volatiles were removed under vacuum to afford a red-orange powder. Three compounds {[Rh(CO)$_2$(*S*-EtSNS)Cl], [H_2EtSNS][Rh(CO)$_2$Cl$_2$] (**5**), and [Rh(CO)(EtSNS)])} were spectroscopically identified as the major components of the crude product. Crystals of compound **5** were obtained by layering hexane onto a solution of the crude product. $^{31}P\{^1H\}$ NMR (161.98 MHz, $CDCl_3$): δ = 16.85 (s, integration 0.75, [Rh(CO)(EtSNS)]), 13.30 (s, integration 1, compound **5**),

12.90 (d, $^2J_{P,P}$ = 15.2 Hz, integration 0,12), 11.44 (d, $^2J_{P,P}$ = 15.2 Hz, integration 0.12, [Rh(CO)$_2$(*S*-EtSNS)Cl]) ppm. FTIR (Diamond crystal HATR): $\tilde{\nu}$ = 2071 (ν_{CO}), 1992 (ν_{CO}) cm^{-1}.

[H$_2$EtSNS][Rh(cod)Cl$_2$] (6): Solid (H$_2$EtSNS)Cl (0.242 g, 0.406 mmol) was added to a solution of [Rh(cod)Cl]$_2$ (0.100 g, 0.203 mmol) in CH_2Cl_2 (20 mL). The resulting orange reaction mixture was stirred for 10 min. Evaporation of the volatiles afforded [H$_2$EtSNS][Rh(cod)Cl$_2$] (**6**) as an orange powder (Yield: 92%). The salt can be recrystallized by layering hexane onto its CH_2Cl_2 solution. ^{1}H NMR (300.13 MHz, $CDCl_3$): δ = 12.70 (br. s, 2 H, N-H), 7.6–7.1 (m, 20 H, Ph), 4.18 (br. m, 8 H, CH_2CH_3 and CH=CH), 2.48 (br. m, 4 H, C*H*H, cod), 1.73 (br. m, 4 H, CH*H*, cod), 1.49 (t, $^3J_{H,H}$ = 7.05 Hz, 6 H, CH_2CH_3) ppm. ^{31}P{^{1}H} NMR (161.98 MHz, $CDCl_3$): δ = 13.6 (s) ppm. $C_{38}H_{44}Cl_2N_3P_2RhS_2$ (842,67): calcd. C 54.16, H 5.26, N 4.99, S 7.61; found C 54.49, H 5.18, N 5.01, S 7.73.

[Rh(CO)(*S*,*N*,*S*-H$_2$EtSNS)][Rh(CO)$_2$Cl$_2$]$_2$ (7): A solution of (H$_2$EtSNS)Cl (0.100 g, 0.17 mmol) in CH_2Cl_2 (10 mL) was added under an atmosphere of nitrogen to a solution of [Rh(CO)$_2$Cl]$_2$ (0.099 g, 0.255 mmol) in CH_2Cl_2 (10 mL). Stirring was continued for 2 h, and the solution color turned to dark red. Evaporation of the volatiles afforded **7** as a red microcrystalline powder (Yield: 91%). ^{1}H NMR (300.13 MHz, [D$_6$]DMSO): δ = 11.08 (br. s, 2 H, N-H), 7.9–7.3 (m, 20 H, Ph), 4.15 (dd, $^3J_{H,H}$ = 6.3 Hz, $^4J_{H,P}$ = 6.3 Hz, 4 H, CH_2CH_3), 1.25 (t, $^3J_{H,H}$ = 6.3 Hz, 6 H, CH_2CH_3) ppm. ^{31}P{^{1}H} NMR (161.98 MHz, $CDCl_3$): δ = 38.2 (s) ppm. $C_{35}H_{32}Cl_4N_3O_5P_2Rh_3S_2$ (1151.26): calcd. C 36.51, H 2.80, N 3.65, S 5.57; found C 36.39, H 2.86, N 3.54, S 5.71. MS (ESI+, MeOH): *m*/*z* (%) = 691.6 (100) [Rh(CO)(H$_2$EtSNS)]$^{2+}$. FTIR (Diamond crystal HATR): $\tilde{\nu}$ = 2064 (m, ν_{CO}), 2011 (m, ν_{CO}), 1990 (s, ν_{CO}), 1985 (s, ν_{CO}), 1961 (m, sh. ν_{CO}) cm^{-1}. FTIR (CH_2Cl_2): $\tilde{\nu}$ = 2074 (s, ν_{CO}[Cl$_2$Rh(CO)$_2$]$^-$), 1998 (s, ν_{CO}[Cl$_2$Rh(CO)$_2$]$^-$), 2014 (m, sh, ν_{CO}Rh–CO) cm^{-1}.

[Rh(CO)(*S*,*N*,*S*′-HEtSNS)PF$_6$ (8): A solution of HEtSNS (0.280 g, 0.50 mmol) in CH_2Cl_2 (10 mL) was added under an atmosphere of nitrogen to a solution of [Rh(CH$_3$CN)$_2$(CO)$_2$]PF$_6$ (0.193 g, 0.50 mmol) in CH_2Cl_2 (10 mL). Stirring was continued for 2 h, and the solution color turned to violet red. Evaporation of the volatiles afforded **8** as a red microcrystalline powder (Yield: 89%). The complex can be recrystallized by layering pentane onto a thf solution of **8** to afford red crystals of **8**·2thf. ^{1}H NMR (300.13 MHz, [D$_6$]DMSO): δ = 11.0 (br. s, 1 H, N-H), 7.7–7.4 (m, 20 H, Ph), 3.67 (m, $^3J_{H,H}$ = 6.2 Hz, 4 H, CH_2CH_3), 1.16 (t, $^3J_{H,H}$ = 6.2 Hz, 6 H, CH_2CH_3) ppm. ^{31}P{^{1}H} NMR (161.98 MHz, $CDCl_3$): δ = 35.0 (s), 19.9 (s) ppm. $C_{31}H_{31}F_6N_3OP_3RhS_2$ (835.55): calcd. C 44.56, H 3.74, N 5.03, S 7.67; found C 44.45, H 3.69, N 4.96, S 7.58. MS (ESI+, MeOH): *m*/*z* (%) = 690.6 (100) [Rh(CO)(HEtSNS)]$^+$. FTIR (Diamond crystal HATR): $\tilde{\nu}$ = 1979 (ν_{CO}) cm^{-1}. FTIR (CH_2Cl_2): $\tilde{\nu}$ = 1994 (ν_{CO}) cm^{-1}.

[Rh(CO)(*S*,*N*,*S*-H$_2$EtSNS)](PF$_6$)$_2$ (9): A solution of [Rh(CH$_3$CN)$_2$(CO)$_2$]PF$_6$ (0.193 g, 0.50 mmol) in CH_2Cl_2 (10 mL) was added under an atmosphere of nitrogen to a solution of (H$_2$EtSNS)PF$_6$ (0.352 g, 0.50 mmol) in CH_2Cl_2 (15 mL). Stirring was continued for 2 h, and the solution color turned to red. Evaporation of the volatiles afforded **9** as an orange microcrystalline powder (Yield: 88%). ^{1}H NMR (300.13 MHz, [D$_6$]DMSO): δ = 11.1 (br. s, 2 H, N-H), 7.8–7.4 (m, 20 H, Ph), 4.15 (m, $^3J_{H,H}$ = 6.2 Hz, 4 H, CH_2CH_3), 1.18 (t, $^3J_{H,H}$ = 6.2 Hz, 6 H, CH_2CH_3) ppm. ^{31}P{^{1}H} NMR (161.98 MHz, $CDCl_3$): δ = 38.2 (s) ppm. $C_{31}H_{32}F_{12}N_3OP_4RhS_2$ (981.52): calcd. C 37.93, H 3.29, N 4.28, S 6.53; found C 37.55, H 3.21, N 4.15, S 6.38. MS (ESI+, MeOH): *m*/*z* (%) = 691.6 (100) [Rh(CO)(H$_2$EtSNS)]$^{2+}$. FTIR (Diamond crystal HATR): $\tilde{\nu}$ = 1996 (ν_{CO}) cm^{-1}. FTIR (CH_2Cl_2): $\tilde{\nu}$ = 2017 (ν_{CO}) cm^{-1}.

[Rh(CO)(*S*,*N*,*S*-HEtSNS)]OTf: A solution of [Rh(CH$_3$CN)$_2$(CO)$_2$]-OTf (0.200 g, 0.37 mmol) in CH_2Cl_2 (10 mL) was added under an atmosphere of nitrogen to a solution of HEtSNS (0.215 g, 0.37 mmol) in CH_2Cl_2 (15 mL). Stirring was continued for 2 h, and the solution color turned to red. Evaporation of the volatiles afforded compound the product as an orange microcrystalline powder (Yield: 87%). ^{1}H NMR (300.13 MHz, [D$_6$]DMSO): δ = 11.0 (br. s, 1 H, N-H), 7.7–7.4 (m, 20 H, Ph), 3.67 (m, $^3J_{H,H}$ = 6.3 Hz, 4 H, CH_2CH_3), 1.16 (t, $^3J_{H,H}$ = 6.3 Hz, 6 H, CH_2CH_3) ppm. ^{31}P{^{1}H} NMR (161.98 MHz, $CDCl_3$): δ = 35.0 (s), 19.9 (s) ppm. $C_{32}H_{31}F_3N_3O_4P_2RhS_3$ (839.65): calcd. C 45.77, H 3.72, N 5.00, S 11.45; found C 45.62, H 3.69, N 4.97, S 11.39. MS (ESI+, MeOH): *m*/*z* (%) = 691.6 (100) [Rh(CO)(HEtSNS)]$^+$. FTIR (Diamond crystal HATR): $\tilde{\nu}$ = 1979 (ν_{CO}) cm^{-1}.

[Rh(CO)(*S*,*N*,*S*-H$_2$EtSNS)](OTf)$_2$: In a Schlenk tube and under an atmosphere of nitrogen, a solution of [Rh(CO)(EtSNS)] (0.200 g, 0.29 mmol) in chloroform (10 mL) was treated with water solution of HOTf (10 mL) in large excess with respect to the rhodium precursor. The yellow solution turned orange-red and a precipitate formed, which was separated by decanting. The two liquid phases were separated, and the organic layer was dried to give an orange-red solid. The two solids were recrystallized from hot methanol to afford the product as an orange microcrystalline powder (Yield: 90%). ^{1}H NMR (300.13 MHz, $CDCl_3$): δ = 11.1 (br. s, 2 H, N-H), 7.8–7.4 (m, 20 H, Ph), 4.15 (m, $^3J_{H,H}$ = 6.3 Hz, 4 H, CH_2CH_3), 1.18 (t, $^3J_{H,H}$ = 6.3 Hz, 6 H, CH_2CH_3) ppm. ^{31}P{^{1}H} NMR (161.98 MHz, [D$_6$]DMSO): δ = 38.2 (s) ppm. $C_{33}H_{32}F_6N_3O_7P_2RhS_4$ (989.73): calcd. C 40.04, H 3.26, N 4.24, S 12.96; found C 39.97, H 3.23, N 4.19, S 12.89. MS (ESI+, MeOH): *m*/*z* (%) = 691.6 (100) [Rh(CO)(H$_2$EtSNS)]$^{2+}$. FTIR (Diamond crystal HATR): $\tilde{\nu}$ = 1995 (ν_{CO}) cm^{-1}.

UV/Vis Titration: The spectra of reference complexes [Rh(CO)-(EtSNS)], [Rh(CO)(HEtSNS)]OTf, and [Rh(CO)(H$_2$EtSNS)]-(OTf)$_2$ were recorded in 1×10^{-3} M dichloromethane solutions (see Figures S4, S5, and S6, respectively; Supporting Information). Purity was previously checked by ^{1}H and ^{31}P{^{1}H} NMR spectroscopy and elemental analysis. A dichloromethane stock solution of [Rh(CO)(EtSNS)] (7×10^{-3} M) was prepared by weight and diluted to 1×10^{-4} M for the UV/Vis titration. KOH aqueous solutions (ca. 0.2 M) were prepared by diluting concentrated Merck Titrisol ampoules and standardized with the reported procedures.[22] The titrant solution of HOTf (ca. 15×10^{-3} M) was prepared by dissolving pure triflic acid (15 μL) in CH_2Cl_2 (10 mL) with the addition of reagent grade methanol (150 μL). Its titre was determined by titrating a suspension of a dichloromethane solution in water (2 mL) with the standard KOH solution using phenolphthalein as indicator. Thirty UV/Vis spectra were collected at different acid/complex ratios (range between 0 and 2.2) by the addition of titrant (25 μL) at each step {concentration of [Rh(CO)(EtSNS)] = 1×10^{-4} M, V_0 = 50 mL}. The spectroscopic data were processed to calculate the protonation constants (pK_a) by means of the program SPECFIT 32 by using the molar absorbance values of the pure protonated complexes as fixed parameters.[23] The wavelength range taken into account in the calculations was limited to 380–600 nm, where the complexes showed major variations in their absorption spectra. The distribution diagram was calculated and plotted using the program HYSS.[24]

X-ray Data Collection, Structure Solution, and Refinement: The intensity data of all compounds were collected at room temperature with a Bruker AXS Smart 1000[25] single-crystal diffractometer

equipped with an area detector by using a graphite monochromated Mo-K_α radiation (λ = 0.71073 Å). Crystallographic and experimental details of the structures are summarized in Table S1 (Supporting Information). When necessary, an empirical correction for absorption was made. The structures were solved by Patterson and Fourier methods and refined by full-matrix least-squares procedures (based on F_o^2)[26] first with isotropic thermal parameters and then with anisotropic thermal parameters in the last cycles of refinement for all the non-hydrogen atoms. The hydrogen atoms were introduced into the geometrically calculated positions and refined riding on the corresponding parent atoms except for the amidic hydrogen atoms and those of the water molecule in [Na(EtSNS)$H_2O]_2$, which were localized in the $2F_o - F_c$ map and refined isotropically. In $(H_2EtSNS)PF_6$ one of the two ethyl groups and the PF_6^- anion were found disordered in two positions; in **2**·1/2thf the thf molecule was found disordered around the twofold axis and in **8**·2thf the PF_6^- anion was found disordered in two positions.

CCDC-671055 (for $H_2EtSNSPF_6$), -671056 {for [Na(EtSNS)$H_2O]_2$}, -671048 (for **1**), -671049 (for **2**), -671050 (for **4**), -671051 (for **5**), -671052 (for **6**), -671053 (for **7**), and -671054 (for **8**), contain the supplementary crystallographic data for this paper. These data can be obtained free of charge from The Cambridge Crystallographic Data Center via www.ccdc.cam.ac.uk/data_request/cif.

Supporting Information (see footnote on the first page of this article): An overall reactivity scheme for complexes derived from Rh(cod) species; $^{31}P\{^1H\}$ NMR spectra in $CDCl_3$ solution of the reaction $[Rh(cod)Cl]_2$ + 2HEtSNS and the reaction $[Rh(CO)_2Cl]_2$ + 2HEtSNS; UV/Vis spectra of compounds [Rh(CO)(EtSNS)], [Rh(CO)(HEtSNS)]OTf, and $[Rh(CO)(H_2EtSNS)](OTf)_2$; crystallographic and experimental details.

Acknowledgments

We thank the Università di Parma for funding this research. We also thank Dr. Pierre Braunstein (Laboratoire de Chimie de Coordination, CNRS Université Louis Pasteur, Strasbourg, France) for access to the NMR spectroscopic facilities of the ULP and Dr. Lionel Allouche (Service Commun de RMN, Université Louis Pasteur, Strasbourg, France) for colleting the MAS-NMR spectra.

[1] a) M. Asti, R. Cammi, D. Cauzzi, C. Graiff, R. Pattacini, G. Predieri, A. Stercoli, A. Tiripicchio, *Chem. Eur. J.* **2005**, *11*, 3413–3419; b) [Rh(CO)(EtSNS)]: ^1H NMR (300 MHz, $CDCl_3$, 25 °C, TMS): δ = 7.48–7.26 (m, 20 H, Ph), 3.75 (qd, $^3J_{H,H}$ = 7.2 Hz, $^4J_{H,P}$ = 3.9 Hz, 4 H, CH_2), 1.19 (t, $^3J_{H,H}$ = 7.2 Hz, 6 H, CH_3) ppm. $^{31}P\{^1H\}$ NMR (400 MHz, $CDCl_3$, 25 °C): δ = 16.6 ppm; c) FTIR (Diamond crystal HATR): $\tilde{\nu}$ = 1951 (ν_{CO}) cm^{-1}.

[2] R. Pattacini, L. Barbieri, A. Stercoli, D. Cauzzi, C. Graiff, M. Lanfranchi, A. Tiripicchio, L. Elviri, *J. Am. Chem. Soc.* **2006**, *128*, 866–876.

[3] In more than 1000 structures of metal compounds containing the PPN^+ cation found in the Cambridge Crystallographic Data Base, the shortest distance (4.047 Å) is reported in: J. Chiba, K. Tanaka, Y. Ohshiro, R. Miyake, S. Hiraoka, M. Shiro, M. Shionoya, *J. Org. Chem.* **2003**, *68*, 331–338.

[4] a) U. Englich, S. Chadwick, K. Ruhlandt-Senge, *Inorg. Chem.* **1998**, *37*, 283–293; b) M. Niemeyer, P. P. Power, *Inorg. Chem.* **1996**, *35*, 7264–7272.

[5] Differently from CH_2Cl_2, the solvent used for the crystallization, it is known that $CHCl_3$ may contain amounts of HCl produced by exposure to light and oxygen.D. G. Hill, *J. Am. Chem. Soc.* **1932**, *54*, 32–40.

[6] a) B. W. Maxey, A. I. Popov, *J. Inorg. Nucleic Chem.* **1970**, *32*, 1029–1032; b) L. Matilainen, M. Leskelae, M. Klinga, *J. Chem. Soc., Chem. Commun.* **1995**, 421–422.

[7] The overall reactivity towards $[Rh(cod)Cl]_2$, solvent-dependent equilibria, and the reaction of complex **1** with CO are depicted in Schemes S1 and S2 (Supporting Information).

[8] The mean value between 180 and 90°(respectively, found in [Au(EtSNS)] and in **1**) is 135° as found in $[Ag(EtSNS)]_2$.

[9] R. Chauvin, *Eur. J. Inorg. Chem.* **2000**, *4*, 577–591.

[10] For recent examples, see: a) V. Miranda-Soto, J. J. Perez-Torrente, L. A. Oro, F. J. Lahoz, M. L. Martin, M. Parra-Hake, D. B. Grotjahn, *Organometallics* **2006**, *25*, 4374–4390; b) S. Cai, G. X. Jin, *Organometallics* **2005**, *24*, 5280–5286; c) J. A. Camerano, M. A. Casado, M. A. Ciriano, C. Tejel, L. A. Oro, *Dalton Trans.* **2005**, *18*, 3092–3100.

[11] V. Amendola, M. Bonizzoni, D. Esteban-Gomez, L. Fabbrizzi, M. Licchelli, F. Sancenon, A. Taglietti, *Coord. Chem. Rev.* **2006**, *250*, 1451–1470.

[12] a) V. L. Goedken, M. L. Vallarino, J. V. Quagliano, *Inorg. Chem.* **1971**, *10*, 2682–2685; b) D. D. J. W. Mercer, H. A. Jenkins, *Inorg. Chim. Acta* **2007**, *360*, 3091–3098.

[13] S. C. Van der Slot, J. Duran, J. Luten, C. Paul, J. Kamer, P. W. N. M. Van Leeuwen, *Organometallics* **2002**, *21*, 3873–3883.

[14] L. Boubekeur, S. Ulmer, L. Ricard, N. Mézailles, P. Le Floch, *Organometallics* **2006**, *25*, 315–317.

[15] During the titration, 30 additions of 25 µL of HOTf dissolved in CH_2Cl_2/CH_3OH were made to 50 mL of solution of [Rh(CO)EtSNS] in neat dichloromethane. Under these conditions, the final quantity of methanol in the titrated solution is negligible (0.02%).

[16] a) T. Fujinaga, I. Sakamoto, *J. Electroanal. Chem.* **1977**, *85*, 185–201; b) J. Bessiere, P. Gagne, *Teintex* **1978**, *43*, 5–12; c) R. L. Benoit, D. Figeys, *Can. J. Chem.* **1991**, *69*, 1985–1988.

[17] a) C. A. Streuli, *Anal. Chem.* **1960**, *32*, 985–987; b) G. Jia, R. H. Morris, *J. Am. Chem. Soc.* **1991**, *113*, 875–883; c) R. H. Morris, *Chem. Eur. J.* **2007**, *13*, 3796–3803.

[18] T. Li, A. J. Lough, C. Zuccaccia, A. Macchioni, R. H. Morris, *Can. J. Chem.* **2006**, *84*, 164–175.

[19] R. A. Begum, D. Powell, K. Bowman-James, *Inorg. Chem.* **2006**, *45*, 964–966.

[20] P. Bhattacharyya, J. D. Woollins, *Polyhedron* **1995**, *14*, 3367–3388.

[21] J. A. Osborn, R. Schrock, *J. Am. Chem. Soc.* **1971**, *93*, 3089–3091.

[22] F. Dallavalle, G. Folesani, R. Marchelli, G. Galaverna, *Helv. Chim. Acta* **1994**, *77*, 1623–1630.

[23] R. A. Binstead, B. Jung, A. D. Zuberbühler, *SPECFIT Global Analysis System*, Version 3.0, Spectrum Software Associates, Marlborough (MA, U.S.A.), **2004**.

[24] L. Alderighi, P. Gans, A. Ienco, D. Peters, A. Sabatini, A. Vacca, *Coord. Chem. Rev.* **1999**, *184*, 311–318.

[25] *SMART Software Users Guide*, Version 5.1, Bruker Analytical X-ray Systems, Madison, WI, **1999**.

[26] a) *SAINT Software Users Guide*, Version 6.0, Bruker Analytical X-ray Systems, Madison, WI, **1999**; b) G. M. Sheldrick, *SADABS*, Bruker Analytical X-ray Systems, Madison, WI, **1999**; c) G. M. Sheldrick, *SHELXL-97*, Program for crystal structure refinement; University of Göttingen, Germany, **1997**.

Received: January 22, 2008
Published Online: April 4, 2008

